DRAFT VERSION FEBRUARY 2, 2008
Preprint typeset using LaTeX style emulateapj

EVIDENCE FOR BLACK HOLE SPIN IN GX 339-4: XMM-NEWTON EPIC-PN AND RXTE SPECTROSCOPY OF THE VERY HIGH STATE

J. M. MILLER[1,2], A. C. FABIAN[3], C. S. REYNOLDS[4], M. A. NOWAK[5], J. HOMAN[5], M. J. FREYBERG[6], M. EHLE[7], T. BELLONI[8], R. WIJNANDS[9], M. VAN DER KLIS[9], P. A. CHARLES[10], W. H. G. LEWIN[5],

Subject headings: Black hole physics – relativity – stars: binaries (GX339−4) – physical data and processes: accretion disks – X-rays: stars

Draft version February 2, 2008

ABSTRACT

We have analyzed spectra of the Galactic black hole GX 339–4 obtained through simultaneous 76 ksec *XMM-Newton*/EPIC-pn and 10 ksec *RXTE* observations during a bright phase of its 2002–2003 outburst. An extremely skewed, relativistic Fe Kα emission line and ionized disk reflection spectrum are revealed in these spectra. Self-consistent models for the Fe Kα emission line profile and disk reflection spectrum rule-out an inner disk radius compatible with a Schwarzschild black hole at more than the 8σ level of confidence. The best-fit inner disk radius of $2-3\ r_g$ suggests that GX 339–4 harbors a black hole with $a \geq 0.8-0.9$ (where $r_g = GM/c^2$ and $a = cJ/GM^2$, and assuming that reflection in the plunging region is relatively small). This confirms indications for black hole spin based on a *Chandra* spectrum obtained later in the outburst. The emission line and reflection spectrum also rule-out a standard power-law disk emissivity in GX 339–4; a broken power-law form with enhanced emissivity inside $\sim 6\ r_g$ gives improved fits at more than the 8σ level of confidence. The extreme red wing of the line and steep emissivity require a centrally–concentrated source of hard X-rays which can strongly illuminate the inner disk. Hard X-ray emission from the base of a jet — enhanced by gravitational light bending effects — could create the concentrated hard X-ray emission; this process may be related to magnetic connections between the black hole and the inner disk. We discuss these results within the context of recent results from analyses of XTE J1650–500 and MCG–6–30–15, and models for the inner accretion flow environment around black holes.

1. INTRODUCTION

Irradiation of an accretion disk orbiting a black hole by a source of hard X-rays can produce a fluorescent Fe Kα emission line, which should bear the signatures of the strong Doppler shifts and gravitational redshifts (Fabian et al. 1989; see also George & Fabian 1991). If the black hole has near-maximal spin ($a \simeq 0.998$, where $a = cJ/GM^2$), the innermost stable circular orbit (ISCO) around the black hole can be as small as $r_{in} = 1.24\ r_g$ (where $r_g = GM/c^2$, note $r_{in} = 6\ r_g$ for $a = 0$); this proximity is expected to produce Fe Kα emission line profiles with strong red wings because of the relative importance of gravitational red-shifts in comparison to Doppler shifts (Laor 1991).

In the X-ray spectra of supermassive black holes in AGN and stellar-mass black holes in Galactic black hole candidates, skewed Fe Kα line profiles have proved to be extremely important diagnostics of the innermost relativistic regime (for AGN, see, e.g., Tanaka et al. 1995; for BHCs, see, e.g., Miller et al. 2002a; for a review see Reynolds & Nowak 2003). In some cases, evidence for black hole spin may be inferred by the line shape (for AGN, see, e.g., Iwasawa et al. 1999, Wilms et al. 2001, Fabian et al. 2003; for BHCs see, e.g., Miller et al. 2002b, Miller et al. 2004, Miniuti, Fabian, & Miller 2004).

GX 339–4 is a recurrent, dynamically-constrained BHC ($M_{BH} \geq 5.8\ M_{\odot}$; Hynes et al. 2003) in which radio jets with $v/c > 0.9$ have recently been observed (Gallo et al. 2004). Herein, we report on the time-averaged 76 ksec *XMM-Newton*/EPIC-pn and 10 ksec *RXTE* spectra of GX 339–4, obtained during a bright phase (near 1 Crab in soft X-rays) of its 2002–2003 outburst.

2. OBSERVATION AND DATA REDUCTION

GX 339–4 was observed with *XMM-Newton* for 75.6 ksec, starting on 29 September 2002 09:06:42 UT (revolution 514). The EPIC-pn camera (Strüder et al. 2001) was operated in "burst" mode to accommodate the high count rate expected during this observation. The "thin" optical blocking filter was used. The data were reduced using the *XMM-Newton* suite SAS version 5.4.1, and the guidelines described in the MPE "cookbook" (see http://wave.xray.mpe.mpg.de/xmm/cookbook). Events were extracted in a stripe in RAWX (31.5–40.5) versus RAWY (2.5–178.5) space. Due to the extremely high source flux back-

[1]Harvard-Smithsonian Center for Astrophysics, 60 Garden Street, Cambridge, MA 02138, jmmiller@cfa.harvard.edu
[2]NSF Astronomy and Astrophysics Fellow
[3]Institute of Astronomy, University of Cambridge, Madingley Road, Cambridge CB3 OHA, England, UK
[4]Department of Astronomy, University of Maryland, College Park, MD, 20742
[5]Center for Space Research and Department of Physics, Massachusetts Institute of Technology, Cambridge, MA 02139–4307
[6]Max-Planck-Institut für Extraterrestriche Physik, Giessenbachstr., D-85748 Garching, DE
[7]*XMM-Newton* SOC, Villafranca Satellite Tracking Station, PO Box 50727, 28080, Madrid, ES & Research and Scientific Support Dept. of ESA, Noordwijk, NL
[8]INAF – Osservatorio Astronomico di Brera, Via E. Bianchi 46, I-3807, Merate, IT
[9]Astronomical Institute "Anton Pannekoek," University of Amsterdam, and Center for High Energy Astrophysics, Kruislaan 403, 1098 SJ, Amsterdam, NL
[11]Department of Physics and Astronomy, University of Southampton, SO17 1BJ, England, UK

ground events were not extracted. The events were then filtered by requiring "FLAG=0" (to reject bad pixels and events too close to chip edges) and "PATTERN $\leq$ 4" (to accept singles and doubles), and the spectral channels were grouped by a factor of 5 to create a spectrum. The appropriate canned burst mode response file was used to fit the spectrum.

RXTE observed GX 339–4 for 9.6 ksec starting on 29 September 2002 09:12:11:28. The data were reduced using the suite LHEASOFT version 5.2. Standard time filtering (primarily, filtering-out the SAA) returned net PCA and HEXTE exposures of 9.3 ksec and 3.3 ksec, respectively. For this analysis, we have only made use of the spectra from PCU-2 (the best-calibrated PCU at the time of writing) and HEXTE-A. Events from all layers of PCU-2 were combined to make spectra; "pcabackest" and the bright source background model were used to make background spectra. We added 0.75% systematic errors to the spectrum from PCU-2 using the tool "grppha". A response matrix (combining rmf and arf files) was generated using "pcarsp". The HEXTE spectral files were made using the standard recipes, and the standard canned responses were used to fit the data. The PCU-2 spectrum was fit in the 2.8–25.0 keV band (standard for *RXTE* analysis; see, e.g., Park et al. 2003), and the HEXTE spectrum was fit on the 20.0–100.0 keV band (the upper bound was fixed by the upper bound over which the ionized disk reflection model is valid). These *RXTE* spectra were fit jointly with an overall normalizing constant allowed to float between them. An edge was added at 4.78 keV with $\tau = 0.1$ to correct for an instrumental Xe edge at this energy in fits to the PCA spectrum.

3. ANALYSIS AND RESULTS

Fits to the *XMM-Newton*/EPIC-pn spectrum, and joint fits to the EPIC-pn and *RXTE* spectra do not yield formally acceptable fits for the models discussed below. A number of sharp, narrow calibration uncertainties remain in the EPIC-pn detector response. For the most part, these appear as absorption lines or edges in the 2–3 keV range (a feature at 2.31 keV appears as an emission line), though similar features are present in the 0.7–2.0 keV band. Most of these features are likely due to Au M-shell edges and Si features in the detector; they are revealed clearly in this observation due to the high signal-to-noise achieved. These narrow-band features do not affect measurements of the Fe Kα emission line profile, but they do affect the overall χ^2 fit statistic. Due to these complications, within this analysis we use the broad-band capacity of *RXTE* to characterize the continuum to serve as a guide for fitting the EPIC-pn data, and reserve detailed joint fits for future work. All fits were made using XSPEC version 11.2.0 (Arnaud 1996). All errors in this work are 90% confidence errors.

The "Laor" model (Laor 1991) describes the line profiles expected around a Kerr black hole. The parameters of this model are the line energy E_{Laor}, the disk emissivity index q (where the emissivity is assumed to have a power-law form of $J(r) \propto r^{-q}$; $q = 3$ is expected for a standard disk), the inner radius of the line emission region r_{in} in units of $r_g = GM/c^2$ (with a lower limit of $r_{in} = 1.235\ r_g$ for $a = 0.998$), the outer line emission radius (fixed to the model limit of $R_{out} = 400\ r_g$), the disk inclination, and the line normalization.

The "pexriv" reflection model (Magdziarz & Zdziarksi 1995) describes reflection from an ionized accretion disk, and does not explicitly include Fe Kα line emission. The important parameters in this model are the reflection fraction f ($f = \Omega/2\pi$),

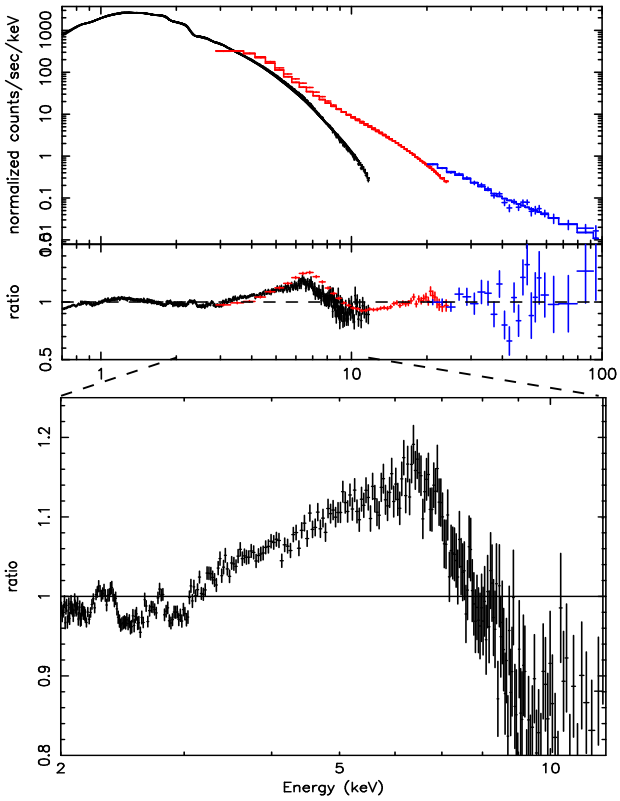

FIG. 1.— Above: the data/model ratio obtained when the *XMM-Newton*/EPIC-pn spectrum (black) and *RXTE*/PCA (red) and HEXTE (blue) spectra are jointly fit with a model consisting of MCD and power-law components. The 4.0–7.0 keV range was ignored when fitting the data, and the spectra were re-binned for clarity. Below: a blow-up of the EPIC-pn spectrum showing the extremely skewed line profile.

the disk temperature, ionization ($\xi = L_X/nr^2$), and inclination, the power-law folding energy (E_{fold}), and the index and normalization of the power-law flux irradiating the disk. The "constant density ionized disk" reflection model (CDID; Ross, Fabian, & Young 1999; Ballantyne, Iwasawa, & Fabian 2001) is a reflection model which includes Fe Kα line emission, and is especially well-suited to high ionization regimes. The relevant parameters of this model are $\log(\xi)$, f, and the index and normalization of the power-law flux irradiating the disk.

These disk reflection spectra are calculated in the co-rotating or fluid frame, and so must be convolved (or, "blurred") with the Laor line element describing the Doppler shifts and gravitational red-shifts expected for an observer in a stationary frame at infinity. In blurring the reflected spectra (and, therefore, the power-law continuum), we linked the parameters of the emission line and blurring function. The disk components were not blurred as the multicolor disk blackbody model (MCD; Mitsuda et al. 1984) — only an approximation to the Shakura & Sunyaev (1973) disk model because it lacks an inner boundary term — may be the best–available model for a disk orbiting a spinning black hole when torques are present at the inner boundary.

3.1. *Fits to the RXTE Spectra*

In fits to the *RXTE* spectra, the equivalent neutral hydrogen column density was fixed at $N_H = 5.3 \times 10^{21}$ cm^{-2} (Dickey & Lockman 1990) using the "phabs" model. No reasonable continuum model gives an acceptable fit to the *RXTE* spectra without the addition of a broad Fe Kα emission line. In the absence of added line components, the best-fit "canonical" MCD plus power-law model gives $\chi^2/\nu = 279.8/74$, the bulk-

motion Comptonization model (Shrader & Titarchuk 1999) gives $\chi^2/\nu = 766.1/74$, and an MCD plus CompTT (Titarchuk 1994) continuum gives $\chi^2/\nu = 284.9/72$ (where ν is the number of degrees of freedom). Adding Gaussian emission line and smeared edge ("smedge") components to the MCD plus power-law model as an approximation to a reflection model, a good fit is achieved ($\chi^2/\nu = 68.2/68$). The parameters measured via this model are: $kT = 0.84^{+0.06}_{-0.04}$ keV, $K_{MCD} = 2800 \pm 600$, $\Gamma = 2.5^{+0.2}_{-0.1}$, $K_{pl} = 2.6 \pm 0.4$, $E_{Gauss} = 5.8^{+0.6}_{-0.8}$ keV, FWHM= 3^{+1}_{-2} keV, $K_{Gauss} = 3^{+3}_{-2} \times 10^{-2}$, EW= 300^{+300}_{-100} eV, $E_{smedge} = 8.7^{+0.6}_{-0.9}$ keV, $\tau = 0.2^{+0.8}_{-0.2}$, and $W_{sm} = 2^{+2}_{-1}$ keV (where K denotes model normalizations, and the "smedge" energy was constrained to lie in the 7.1–9.3 keV range).

Fits were also made with blurred CDID and pexriv models. Blurring the models for the $1.24-400$ r_g range and assuming a power-law emissivity of $q = 3.0$, we found that the data are consistent with strong reflection ($f \simeq 1$) from a highly ionized inner disk ($\log(\xi) = 4.3-4.4$). A line equivalent width of $EW \simeq 200 \pm 80$ eV was meausured using the pexriv model.

3.2. *Fits to the XMM-Newton/EPIC-pn Spectrum*

Due to the hints of an extremely skewed spectrum found with *RXTE*, we began by fitting more physical models to the *XMM-Newton*/EPIC-pn spectrum. Broad line residuals extend down to $\sim$3 keV regardless of whether models with additive components or single-component (e.g., bulk motion Comptonization) models are used to fit the continuum, which indicates that the continuum does not strongly affect the red wing of the line. The first model we considered included MCD and power-law continuum components, with added Laor line and smeared edge components. The power-law index was constrained to lie within $\Delta(\Gamma) \leq 0.1$ of the *RXTE*-measured values. With this model, we measure the following values: $N_H = 5.1 \pm 0.1 \times 10^{21}$ cm^{-2}, $kT = 0.76 \pm 0.01$ keV, $K_{MCD} = 2300^{+100}_{-200}$, $\Gamma = 2.60_{-0.05}$, $K_{pl} = 2.2^{+0.3}_{-0.1}$, $E_{Laor} = 6.97_{-0.20}$ keV, $q = 5.5^{+0.5}_{-0.1}$, $r_{in} = 2.1^{+0.2}_{-0.1}$ r_g, $i = 11^{+5}_{-1}$ deg., $K_{laor} = 7.7^{+0.5}_{-1.5} \times 10^{-2}$, $EW_{Laor} = 200^{+10}_{-40}$ eV, $E_{sm} = 7.9^{+0.1}_{-0.4}$ keV, $\tau = 0.6^{+0.4}_{-0.1}$, and a smeared edge width of $W = 1.0 \pm 0.3$ keV. An inner radius of $r_{in} = 6$ r_g (as per a black hole with $a = 0$) is excluded at more than the 8σ level of confidence, as is a standard emissivity index of $q = 3$. This model gives $\chi^2/\nu = 3456.5/1894$; the formally unacceptable fit is due to the calibration problems discussed in Section 3.0. A joint fit to the *XMM-Newton*/EPIC-pn and *RXTE* spectra using these continuum parameters is shown in Figure 1. These spectral parameters, and the timing properties of the source at the time of this observation (Homan et al. 2004), indicate that GX 339–4 was observed in the "very high" state.

Using this model, we measure an unabsorbed flux of 2.1×10^{-8} erg cm^{-2} s^{-1} in the 0.5–10.0 keV band; the power-law contributes 35% of this flux. The total line flux is measured to be 5.3×10^{-10} erg cm^{-2} s^{-1}, or 8.4×10^{-2} ph cm^{-2} s. It should be noted that the best fit without a line component gives $\chi^2/\nu = 7552/1902$. Clearly, a broad line component is required at far more than the 8σ level of confidence.

Models which allow the disk emissivity law to assume a broken power-law form, with $J(r) \propto r^{-q_{in}}$ within radius r_q, and $J(r) \propto r^{-q_{out}}$ outside of r_q, yield statistically improved fits over models assuming simple power-law emissivity laws at more than the 8σ level of confidence.

Allowing for a broken power-law form for the emissivity and a blurred CDID reflection model, we measure: $N_H = 5.5 \pm 0.1 \times 10^{21}$ cm^{-2}, $kT = 0.79 \pm 0.01$ keV, $K_{MCD} = 1860 \pm 20$,

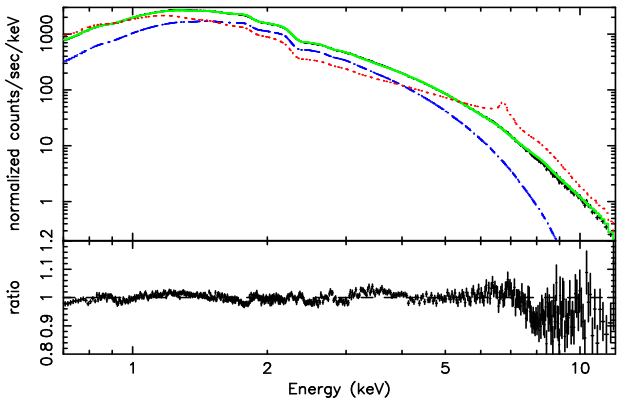

FIG. 2.— The EPIC-pn spectrum of GX 339–4 fit with a relativistically blurred reflection model, with data/model ratio shown below. The total spectrum is shown in green, the disk component in blue, and the CDID reflection model is shown in red (prior to blurring). The data were re-binned for clarity.

$\Gamma = 2.61^{+0.09}_{-0.01}$, $K_{CDID} = 2.8 \pm 0.2 \times 10^{-26}$, $\log(\xi) = 4.5^{+0.5}_{-0.1}$, $f = 2.0_{-0.2}$, $r_{in} = 2.9 \pm 0.1$, $q_{in} = 5.5^{+0.5}_{-0.7}$, $q_{out} = 3.0^{+0.6}$, $r_q = 7 \pm 2$ r_g, and $i = 11^{+5}_{-1}$ deg., for $\chi^2/\nu = 3887.3/1895$. This fit to the EPIC-pn spectrum is shown in Figure 2.

Fits with a blurred pexriv model with a broken power-law emissivity ($\xi = 3.0 \times 10^4$, $kT_{disk} = 1.0$ keV as per Young et al. 2001, $E_{fold} = 200$ keV, $r_q = 6$ r_g, and $q_{out} = 3$ were fixed) yielded the following fit parameters: $N_H = 5.3 \pm 0.1 \times 10^{21}$ cm^{-2}, $kT = 0.76 \pm 0.01$ keV, $K_{MCD} = 2200 \pm 300$, $\Gamma = 2.61^{+0.09}_{-0.01}$, $K_{PL,pexriv} = 1.5 \pm 0.1$, $i = 12^{+4}_{-2}$ deg., $E_{laor} = 6.97_{-0.07}$ keV, $r_{in} = 2.1^{+0.5}_{-0.3}$, $q_{in} = 5.5^{+0.5}_{-0.2}$, $K_{laor} = 7.2 \pm 0.3 \times 10^{-2}$, $EW = 210^{+60}_{-60}$ eV, and $f = 1.0^{+0.5}_{-0.1}$, giving $\chi^2/\nu = 3481.3/1896$.

The measured inner disk color temperature and high disk ionizations are expected in the very high state. Reflection fractions greater than unity might be taken as indications of light bending effects. All fits show negative residuals above $E \simeq 8.0-8.5$ keV. Reflection models predict a steeper continuum and also account for ionized Fe K-shell absorption in this range. The observed residuals can be corrected with a phenomenological smeared edge component "τ" $\simeq 0.5$,but would be better modeled by refinements to reflection models.

At high mass accretion rates, disks around black holes likely extend to the ISCO. Although the Laor model assumes maximal black hole spin, it is likely broadly valid over a range of high spin parameters. Assuming that $r_{in} = r_{ISCO}$ (equivalent to assuming that the inner disk drags matter in the plunging region minimally; see Krolik & Hawley 2002, Reynolds & Begelman 1997, and Young, Ross, & Fabian 1998); equation 2.21 in Bardeen, Press, & Teukolsky (1972) may be used to estimate the spin parameter of the black hole in GX 339–4. Using this procedure, the line and reflection fits detailed above suggest that GX 339–4 harbors a black hole with $a \geq 0.8-0.9$.

4. DISCUSSION

We have discovered an extremely skewed Fe Kα emission line in an *XMM-Newton*/EPIC-pn spectrum of the Galactic black hole GX 339–4. Spectral fits with the Laor relativistic disk line model and a phenomenological continuum, and with the Laor model and self-consistent blurred disk reflection models, provide tight constraints on the nature of the black hole and inner accretion flow in GX 339–4. Our fits indicate that the inner disk likely extends to $r_{in} = 2-3$ r_g, translating to a black hole spin parameter of $a \geq 0.8-0.9$. Moreover, an enhanced inner disk emissivity index of $q = 4.8-6.0$ is required within

$5-9\ r_g$. Fits with the same models which fix either $r_{in} = 6.0\ r_g$ (as per an $a = 0$ Schwarzschild hole) or $q = 3.0$ (as per a standard disk), are more than 8σ worse than the best-fit values summarized here and detailed in the previous section.

X-ray spectroscopy of XTE J1650−500 (Miller et al. 2002b, Miniutti, Fabian, & Miller 2003) and MCG–6-30-15 (Wilms et al. 2001, Fabian et al. 2002) has revealed remarkably similar line profiles and inner disk emissivity properties; both XTE J1650−500 and MCG–6-30-15 may have spin parameters which are similar to GX 339–4. Comparisons of the timing phenomena observed in stellar-mass Galactic black holes and Seyfert galaxies have shown that noise properties may simply scale with mass (Uttley & McHardy 2001). It has also recently been shown that Galactic black holes may have AGN-like warm absorbers (Miller et al. 2004). Our results extend these findings in that they suggest that — at least in certain states — details like enhanced inner disk emissivity are likely similar.

The models we have considered not only constrain the black hole spin parameter, but also the nature of the inner accretion flow geometry. The inner disk must be strongly illuminated by a centrally-concentrated source of hard X-rays. Miniutti & Fabian (2003) have calculated the effects of light bending on Fe Kα line variability. This model can explain the complex time variability seen in MCG–6-30-15, and appears to describe the behavior of the line strength in XTE J1650−500 remarkably well (Miniutti, Fabian, & Miller 2004; Rossi et al. 2003). The light bending model assumes a power-law source of hard X-ray emission above the black hole which moves "vertically" along the black hole and inner disk angular momentum axis. While models for jets in Galactic black holes require that X-ray emission be focused away from the disk (see, e.g., Markoff, Falcke, & Fender 2001), at the base of the jet the flow is less relativistic and the beaming therefore less extreme. It is possible that synchrotron self-Compton emission from the base of a jet may be focused onto the inner disk by light bending (this would represent an extension to the jet reflection considered by Markoff & Nowak 2004). This does not rule-out additional hard X-ray emission from a corona.

Heightened inner disk emissivity of the kind seen in GX 339–4 can plausibly be explained by the dissipation of the black hole's rotational energy via magnetic connections to the inner disk (Blandford & Znajek 1977; see also Gammie 1999 and Li 2003). The emissivity we have measured is above that predicted by magnetic connections to matter in the plunging region ($q = 7/2$, Agol & Krolik 2000), though it is possible this process could also be at work. It is possible that such processes and the putative illumination of the inner disk region by the base of a jet might be intimately related; indeed, the extraction of black hole spin energy is often invoked as a possible means of powering relativistic jets in AGN.

We are grateful for thoughtful comments of the anonymous referee. JMM gratefully acknowledges support from the NSF through its Astronomy and Astrophysics Postdoctoral Fellowship program. This work is based on observations obtained with *XMM-Newton*, an ESA science mission with instruments and contributions directly funded by ESA Member States and the USA (NASA).

REFERENCES

Agol, E., & Krolik, J. H., 2000, ApJ, 528, 161
Arnaud, K. A., 1996, ADASS V, eds. G. Jacoby and J. Barnes, ASP Conf. Series 101, 17
Ballantyne, D. R., Iwasawa, K., & Fabian, A. C., 2001, MNRAS, 323, 506
Bardeen, J. M., Press, W. H., & Teukolsky, S. A., 1972, ApJ, 178, 347
Blandford, R. D., & Znajek, R. L., 1977, MNRAS, 179, 433
Dickey, J. M., & Lockman, F. J., 1990, ARA& A, 28, 215
Fabian, A. C., Rees, M. J., Stella, L., & White, N. E., 1989, MNRAS, 239, 729
Fabian, A. C., et al. 2002, MNRAS, 335, L1
Gammie, C., 1999, ApJ, 522, L57
George, I. M., & Fabian, A. C., 1991, MNRAS, 249, 352
Hynes, R. I., Steeghs, D., Casares, J., Charles, P. A., & O'Brien, K., 2003, ApJ, 583, L95
Homan, J., et al. 2004, in prep.
Iwasawa, K., Fabian, A. C., Young, A. J., Inoue, H., & Matsumoto, C., 1999, MNRAS, 306, L19
Krolik, J. H., & Hawley, J. F., 2002, ApJ, 573, 754
Laor, A., 1991, ApJ, 376, 90
Li, L., 2003, PhRvD, 67, 4007
Magdziarz, P., & Zdziarski, A. A., 1995, MNRAS, 273, 837
Markoff, S., Falcke, H., & Fender, R. P., 2001, A & A, 372, L25
Markoff, S., & Nowak, M., 2004, ApJ, subm.
McClintock, J. E., & Remillard, R. A., 2003, in "Compact Stellar X-ray Sources" ed. W. H. G. Lewin and M. van der Klis, Cambridge (Cambridge University Press)
Merloni, A. A., Fabian, A. C., & Ross, R. R., 2000, MNRAS, 313, 193
Miller, J. M., et al. 2002a, ApJ, 578, 348
Miller, J. M., et al. 2002b, ApJ, 560, L69
Miller, J. M., et al. 2004, ApJ, in press, astro-ph/0307394
Miniutti, G., Fabian, A. C., & Miller, J. M., 2004, MNRAS, subm., astro-ph/0311037
Mitsuda, K., et al. 1984, PASJ, 36, 741
Park, S. Q., et al. 2004, ApJ, in press, astro-ph/0308363
Reynolds, C. S., & Begelman, M. C., 1997, ApJ, 488, 109
Reynolds, C. S., & Nowak, M. A., 2003, Physics Reports, 377, 389
Ross, R. R., Fabian, A. C., & Young, A. J., 1999, MNRAS, 306, 461
Rossi, S., Homan, J., Miller, J. M., & Belloni, T., 2003, to appear in the Proc. of the BeppoSAX Symposium "The Restless High Energy Universe" eds. E. van den Heuvel, J. In 't Zand, and R. Wijers, astro-ph/0309129
Shakura, N. I., & Sunyaev, R. A., 1973, A& A, 86, 121
Shimura, T., & Takahara, F., 1995, ApJ, 445, 780
Shrader, C., & Titarchuk, L., 1999, ApJ, 521, L91
Strüder, L., et al. 2001, A& A, 365, L18
Tanaka, Y., et al., 1995, Nature, 375, 650
Titarchuk, L., 1994, ApJ, 434, 570
Uttley, P., & McHardy, I., 2001, MNRAS, 363, L26
Wilms, J., Reynolds, C. S., Begelman, M. C., Reeves, J., Molendi, S., Staubert, R., & Kendziorra, E., 2001, MNRAS, 328, L27
Young, A. J., Ross, R. R., & Fabian, A. C., 1998, MNRAS, 300, L11
Young, A. J., Ross, R. R., Fabian, A. C., & Tanaka, Y., 2001, MNRAS, 325, 1045